ORIGINAL ARTICLE

JOURNAL OF PANCREATOLOGY®

OPEN

Exploring the role of YAP1 and TAZ in pancreatic acinar cells and the therapeutic potential of VT-104 in pancreatic inflammation

Kevin Lopez[a], Janice J. Deng[a], Yi Xu[a], Francis E. Sharkey[b], Pei Wang[a,*], Jun Liu[a,*]

Abstract

Background: Increasing evidence has linked the Hippo pathway with the fibroinflammatory diseases. However, the detailed roles of key hippo components in pancreatic inflammatory diseases still remain unclear.

Methods: A series of genetic knockout mice were generated targeting the key components of Hippo pathway to examine the individual effects of YAP1 and TAZ on pancreatic inflammation. Hematoxylin and eosin (H&E) staining, immunohistochemistry, and immunofluorescence staining were performed to evaluate the pancreas tissue from mice with various genotypes. The therapeutic potential of a recently developed YAP1/TAZ inhibitor VT-104 was also evaluated in our mouse model.

Results: Mice with acinar-specific knockout of YAP1/TAZ did not exhibit any histological abnormalities in the pancreas. LATS1/2 deficiency induced acinar to ductal metaplasia, immune cell infiltration, and fibroblast activation, which were rescued by the homozygous knockout YAP1, but not TAZ. Additionally, treatment with VT-104 also decreased pathological alterations induced by deletions of LATS1 and LATS2 in acinar cells.

Conclusion: Our findings highlight the critical role of YAP1 in modulating pancreatic inflammation and demonstrate that VT-104 holds therapeutic potential to mitigate pancreatitis-associated pathological manifestations. Further exploration is necessary to unravel the underlying mechanisms and translate these insights into clinical applications.

Keywords: Fibrosis, Hippo pathway, Inflammation, Pancreatitis, TAP1/TAZ

Introduction

Pancreatitis is a disease characterized by pancreatic inflammation with either acute or chronic manifestation.[1] Recently, a direct link between recurrent acute pancreatitis (AP) and chronic pancreatitis (CP) in patients has been established and is thought to be a progression of the same disease rather than independently distinct disease types.[2] In addition, retrospective analysis of patients with a single event of AP has shown an increased risk for development of recurrent episodes of AP.[3] Furthermore, pancreatitis is the leading cause of gastrointestinal-related hospital admissions, proving to be a burdensome disease on people and hospitals.[4] This raises the important question of how aberrant activation of the fibroinflammatory response in the pancreas can occur and how it may be controlled.

The Hippo pathway, initially discovered in Drosophila, is highly conserved in mammals. It uses a kinase cascade including mammalian Ste20-like kinases 1/2 (MST1/2) and Large tumor suppressor 1/2 (LATS1/2) to control the downstream Yes-associated protein 1 (YAP1) and transcriptional co-activator with PDZ-binding motif (TAZ). Mechanistically, active MST1/2 phosphorylates LATS1/2 to enable them to further phosphorylate Yap1/Taz. Phosphorylation of YAP1/TAZ inhibits their cytosol-to-nuclear translocation while promoting cytosolic retention/sequestration and ubiquitination-mediated degradation and/or glycosylation to prevent downstream transcriptional activation.[5] The hippo pathway can be inactivated by various events such as growth factor stimulation and disruption of cell-cell contact. Under these scenarios, LATS1/2 are inactivated and no longer phosphorylate YAP1/TAZ thus allowing for YAP1/TAZ to translocate to the nucleus and participate in transcriptional regulation via interactions with TEA domain DNA-binding family members (TEAD1-4).[6,7] YAP1 and TAZ were extensively investigated in cancers because they have been best known for their roles in regulating cell survival and proliferation.[8] More recently, emerging evidence highlighted the importance of Hippo pathway to modulate innate immune response.[9] In our previous study, we discovered the direct role of the Hippo signaling pathway in activation of the fibroinflammatory response within acinar cells and how uncontrolled expression of YAP1/TAZ leads to development of a pancreatitis-like phenotype.[10] Consistent with our observation, the other group also reported that the inactivation of Hippo pathway cooperated with PI3K aberrant activation in acinar cells to induce CP.[11] Though the Hippo pathway's direct role in the fibroinflammatory response is undoubtedly important, many questions remain unanswered in the direct, independent roles of each YAP1 and TAZ, respectively, in development of pancreatitis-like phenotypes.

Therefore, in this study, we generated novel genetically engineered mouse models to evaluate the direct roles of each YAP1

[a]Department of Cell Systems & Anatomy, University of Texas Health Science Center at San Antonio, San Antonio, TX, [b]Department of Pathology and Laboratory Medicine, University of Texas Health Science Center at San Antonio, San Antonio, TX

Supplemental digital content is available for this article.

Data sharing not applicable to this article as no datasets were generated or analyzed during the current study.

* Corresponding author: Jun Liu, Department of Cell Systems & Anatomy, University of Texas Health Science Center at San Antonio, 7703 Floyd Curl Drive, San Antonio, TX 78229. E-mail: liuj8@uthscsa.edu; Pei Wang, e-mail: wangp3@uthscsa.edu

Journal of Pancreatology (2025) 8:1

Received: 9 October 2023; Accepted 5 January 2024.

Published online 17 January 2024

http://dx.doi.org/10.1097/JP9.0000000000000170

and TAZ, respectively, in the activation of the fibroinflammatory response and the induction of pancreatitis-like phenotypes via the Hippo pathway. In addition, we also evaluated YAP1 and TAZ's individual roles, through Hippo signaling, for the induction of acinar to ductal metaplasia (ADM). Finally, we determined the efficacy of pharmaceutical inhibition of YAP1/TAZ transcriptional activities using the novel YAP1/TAZ-TEAD-complex inhibitor, VT-104,[12] to determine its ability to rescue pancreatitis-associated phenotypes induced by Hippo dysregulation.

Materials and methods

Generation of conditional knockout mice

All animal study protocols were approved by the University of Texas Health San Antonio Animal Care and Use Committee. Ptf1a$^{Cre\text{-}ERTM}$ mice (The Jackson Laboratory, Bar Harbor, ME; stock number: 019378) and R26R-EYFP mice (The Jackson Laboratory; stock number: 006148) were obtained from Hebrok Lab. Lats1$^{fl/fl}$ and Lats2$^{fl/fl}$ mice were kindly provided by Dr Randy L. Johnson. Yap1$^{fl/fl}$ and Taz$^{fl/fl}$ mice were kindly provided by Dr Eric N. Olson. We generated (1) Ptf1a$^{CRE\text{-}ER}$ Rosa26$^{LSL\text{-}YFP}$ mice (P), (2) Ptf1a$^{CRE\text{-}ER}$ Lats1$^{fl/fl}$ Lats2$^{fl/fl}$ Rosa26$^{LSL\text{-}YFP}$ mice (PL), (3) Ptf1a$^{CRE\text{-}ER}$Yap1$^{fl/fl}$ Taz$^{fl/fl}$ Rosa26$^{LSL\text{-}YFP}$ mice (PTY), (4) Ptf1a$^{CRE\text{-}ER}$ Lats1$^{fl/fl}$ Lats2$^{fl/fl}$ Yap1$^{fl/fl}$ Taz$^{fl/fl}$ Rosa26$^{LSL\text{-}YFP}$ mice (PLTY), (5)Ptf1a$^{CRE\text{-}ER}$ Lats1$^{fl/fl}$ Lats2$^{fl/fl}$ Yap1$^{+/fl}$ Taz$^{+/fl}$ Rosa26$^{LSL\text{-}YFP}$ mice (PLT^{Hert}Y^{Hert}), (6) Ptf1a^{CreER} Lats1$^{fl/fl}$ Lats2$^{fl/fl}$ Yap1$^{fl/fl}$ Rosa26$^{LSL\text{-}YFP}$ mice (PLY), and (7) Ptf1a^{CreER} Lats1$^{fl/fl}$ Lats2$^{fl/fl}$ TAZ$^{fl/fl}$ Rosa26$^{LSL\text{-}YFP}$ mice (PLT). All offspring were genotyped by polymerase chain reaction (PCR) of genomic DNA from the toe with primers specific for the Ptf1aCre-ER, Rosa26LSL-YFP, Lats1, Lats2, Yap1, and Taz transgenes (Additional Table 1, http://links.lww.com/JP9/A46) following Jackson Lab's protocol. To induce the conditional knockout, 6- to 12-week-old mice were orally administered with 180 mg/kg of tamoxifen (TAM) (T5648-5G; Sigma-Aldrich, St. Louis, MO) for 5 days, which was dissolved in corn oil (C8267; Sigma-Aldrich). PCR was used for validation of knockout alleles.

VT-104 administration

VT-104, generously supplied by Vivace Therapeutics (San Mateo, CA), was prepared as previously described.[12] PL mice were orally administrated TAM to knockout Lats1&2 as described earlier and VT-104 treatment was started 72 hours after the final TAM administration. A daily dose of VT-104 at 4 mg/kg was administered orally, with the control group receiving the vehicle solvent. On day 9 following the initial VT-104 administration, the mice were humanely euthanized. Pancreatic tissue sections were stained with hematoxylin and eosin (H&E) to quantify the severity of inflammation.

H&E staining, immunofluorescence, and immunohistochemistry staining

Mice were euthanized, and pancreata were dissected into ice-cold phosphate-buffered saline (PBS). For histological examination, mice pancreata were fixed in 4% paraformaldehyde (PFA) overnight at 4°C and then processed for paraffin embedding. Sections were cut at 5 µm and then used for H&E staining or immunostaining. Primary and secondary antibodies used in this study are listed in Additional Table 2, http://links.lww.com/JP9/A47, and Additional Table 3, http://links.lww.com/JP9/A48. For immunohistochemistry (IHC) staining, tissues were deparaffinized, rehydrated, and immersed and heated in a citrate-based antigen unmasking solution (H300; Vector, Burlingame, CA) for 30 minutes, followed by treatment with 3% hydrogen peroxide to quench endogenous peroxidase activity. Sections were blocked with 5% donkey serum in 0.1% Tris buffered saline with Tween 20 (TBST) for 1 hour at room temperature and then incubated with primary antibody at 4°C overnight. Biotin-labeled secondary antibodies and Streptavidin-Horseradish peroxidase were applied to amplify the target antigen signal, and then sections were developed with DAB substrate (K3468; Dako, Santa Clara, CA), followed by counterstaining with hematoxylin (Biocare Medical, Pacheco, CA). Finally, sections were covered with poly-Mount medium (category no. 08381; Polysciences, Warrington, PA). For immunofluorescence staining, frozen sections were blocked with 10% donkey serum plus 1% bovine serum albumin (BSA) in phosphate-buffered saline with Tween 20 (PBST) for 1 hour at room temperature. Sections were incubated with primary antibodies at 4°C overnight followed by incubation with the fluorescent-conjugated secondary antibodies for 1 hour at room temperature. Sections were covered with a drop of ProLong Gold anti-fade reagent with 4',6-diamidino-2-phenylindole (DAPI) (P36935; Invitrogen, Carlsbad, CA) for observation. All images were obtained with a Microsystems DMI6000 B microscope and microscope software (Leica Microsystems, Buffalo Grove, IL). The lobular integrity, acinar atrophy, and immune infiltration were assessed to evaluate pancreas damages with H&E staining. The immunofluorescent data were quantified using Fiji by ImageJ. For all immunofluorescent quantification, each mouse had 4 representative 20× magnification fields that were captured and averaged together for each respective mouse. Each image was normalized using the thresholding tool to mitigate background signal. For F4/80 and α-smooth muscle actin (SMA) quantification, the data were presented as average fluorescent intensity per square micron. For total ADM counts, each cytokeratin 19+ (CK19+) amylase+ cell was hand-counted per 20× field and averaged together, per mouse.

Statistical analysis

The sample size and number of replicates were determined based on the prior experiments that uncovered Hippo's role in the pancreatic fibroinflammatory response. The mean and standard error of the mean (SEM), and 2-tailed Student *t* test were calculated using Prism by Graphpad. *P* values <.05 were considered statistically significant. The data were presented as mean ± SEM for quantitative analyses. The numbers of mice used per experiment were indicated.

Results

Deletion of YAP1/TAZ in acinar cells does not induce abnormal or pancreatitis-like phenotype long term

Previously, we evaluated the effects of homozygous YAP1 and TAZ deletions in adult mice acinar cells and determined that no abnormal phenotypes or pathologies arose from loss of YAP1/TAZ genes within 2 weeks after TAM administration.[10] However, whether YAP/TAZ deletion has long-term effects on pancreas homeostasis was not clear. To answer this, we administered TAM daily for 5 consecutive days by oral gavage at the concentration of 180 mg/kg to delete the floxed alleles in acinar cells of the *Ptf1a^{CreER}Yap1$^{fl/fl}$Taz$^{fl/fl}$Rosa26$^{LSL\text{-}YFP}$* (PTY) mice (Fig. 1A). Then, we sacrificed the mice at 4 months post-TAM administration. Histological analysis by H&E stain revealed no abnormalities of the pancreatic tissues (n = 6) (Fig. 1B). In conclusion, these data suggest that YAP1/TAZ are dispensable for the long-term homeostasis of acinar cells under physiological conditions.

Heterozygous YAP1/TAZ knockout in acinar cells does not rescue Lats1/2 knockout–induced pancreatic damage and inflammation

Our previous study found that homozygous YAP1 and TAZ knockout in Lats1/2-null acinar cells in adult mice rescued pancreatic damage and inflammation.[10] In developing pancreas,

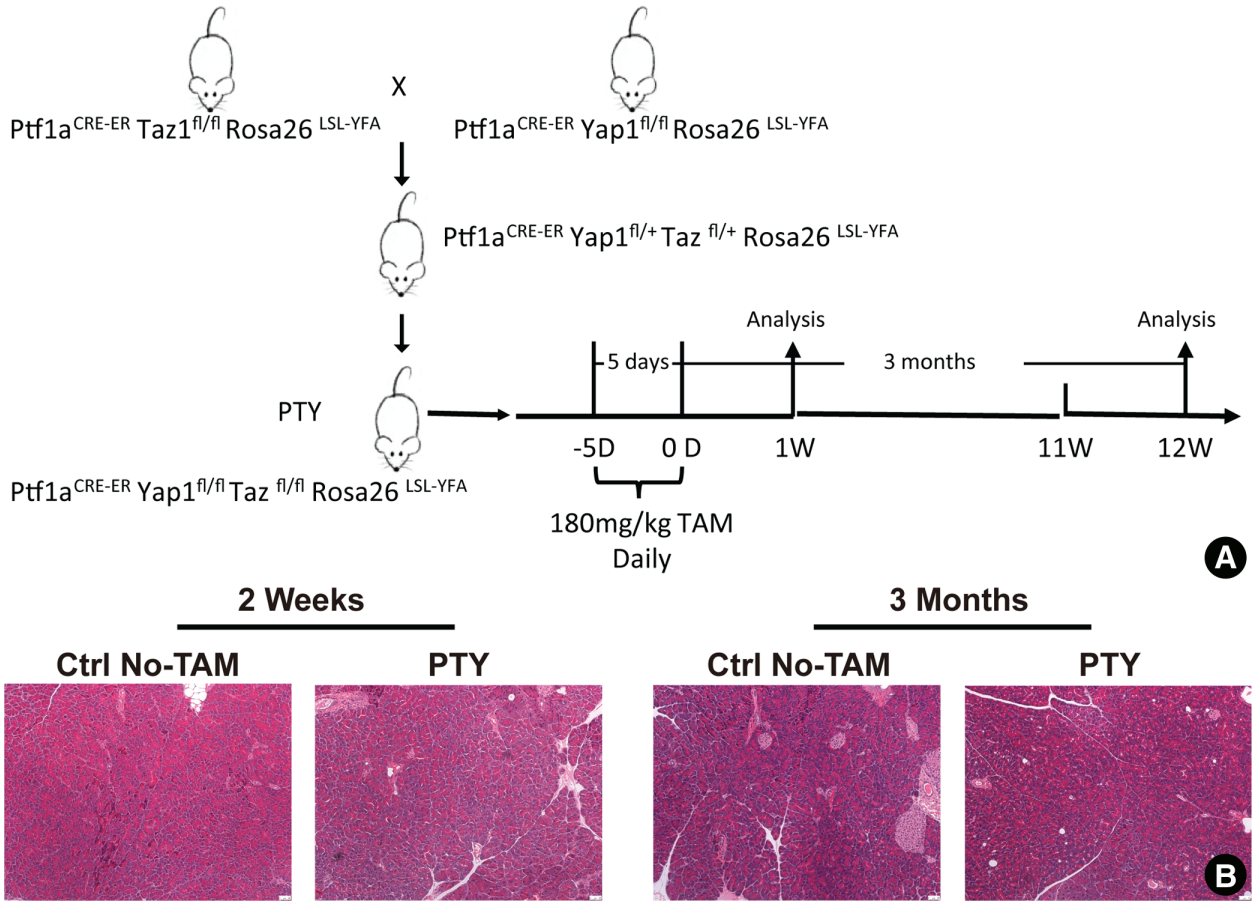

Figure 1. Acinar-specific knockout of YAP1 and TAZ did not disturb pancreas homeostasis under normal conditions. (A) The schema of experimental procedure. (B) The representative H&E staining images of the pancreas collected from the mice treated as indicated. H&E = hematoxylin and eosin, PTY = Ptf1a^{CRE-ER}Yap1$^{fl/fl}$ Taz$^{fl/fl}$ Rosa26$^{LSL-YFP}$ mice, TAM = tamoxifen.

heterozygous YAP1 knockout largely reversed the defects triggered by Hippo deficiency.[13] To confirm the similar effect in adult pancreas, we analyzed the pancreas of heterozygous YAP1 and TAZ knockout in Lats1/2-null acinar cells (*Ptf1a^{CreER}Lats1$^{fl/fl}$Lats2$^{fl/fl}$Yap1$^{fl/+}$Taz$^{fl/+}$Rosa26$^{LSL-YFP}$*, PLThYh) on pancreatic damage and inflammation (Additional Fig. 1, http://links.lww.com/JP9/A43). As expected, we did not observe abnormality in control mice without TAM administration by H&E stain (n = 3) (Fig. 2A). The *Ptf1a^{CreER}Lats1$^{fl/fl}$Lats2$^{fl/fl}$Rosa26$^{LSL-YFP}$* (PL) mice also received the TAM administration. Histological analyses at 7 days post-TAM administration by H&E stain revealed severe pancreatic damage of PLThYh mice (n = 7) that was indistinguishable from the defects observed in PL mice (n = 5) (Fig. 2A). Immunofluorescent staining demonstrated robust F4/80+ macrophage infiltration and fibroblast activation, measured by α-SMA staining, at similar levels in both PL and PLThYh mice (Fig. 2B). Previously, we have demonstrated that Hippo disruption did not induce cell-autonomous proliferation but primed acinar cells to exogenous pro-proliferative stimuli.[10] Therefore, the increased proliferation in the pancreas of Lats1/2 knockout mice is the secondary consequence inflammation response. The IHC stain of marker of proliferation Ki67 did not detect distinguishable differences between PL and PLThYh mice (Fig. 2C). Further immunofluorescent staining of amylase and CK19 revealed extensive, indistinguishable levels of ADM in the pancreas from both PL and PLThYh mice (Fig. 2D). Altogether, the phenotypes observed in PL and PLThYh mice demonstrated inability of YAP1 and TAZ haplotypes to rescue pancreatic damage and inflammation induced by Hippo-pathway disruptions in adult mice acinar cells.

Homozygous YAP1 knockout rescues of pancreatic inflammation and ADM induced by acinar cell–specific Lats1/2 deletions

Although some early studies suggested the redundant functions of YAP1 and TAZ,[14] emerging evidence suggests that they may play synergistic or even opposing roles in different biological contexts.[15] In order to evaluate the contributions of YAP1 activation on pancreatic inflammation induced by acinar-specific Lats1/2-knockout in adult mice pancreas, *Ptf1a^{CreER}Lats1$^{fl/fl}$Lats2$^{fl/fl}$Yap1$^{fl/fl}$Rosa26$^{LSL-YFP}$* (PLY) mice were created (Additional Fig. 1, http://links.lww.com/JP9/A43) and administered TAM as previously described to simultaneously delete LATS1/2 and YAP1 in acinar cells. Upon histological analysis by H&E stain at day 6 post-TAM administration, PLY mice (n = 6) showed a near complete resolution of overall pancreatic damage and inflammation compared to PL mice (n = 3), though containing minor sporadic lesions (Fig. 3A). Next, we evaluated the status of nuclear/cytosolic YAP1 and TAZ using IHC, which was consistent with genotyping for PL and PLY mice. In the PL pancreas, strong nuclear YAP1 and TAZ expression was observed in acinar cells (Fig. 3B). In PLY pancreas, non-damaged areas showed the absence of nuclear and cytosolic YAP1, while nuclear and cytosolic expression of TAZ persisted (Fig. 3B). Interestingly, all small sporadic lesions observed in PLY mice showed strong nuclear YAP1 expression, suggesting incomplete knockout of YAP1 (Additional Fig. 2A, http://links.lww.com/JP9/A44). In addition, the PLY pancreas had reduced expression of downstream YAP1 target SPP1 compared to PL mice (Fig. 3B), further supporting the successful deletion of

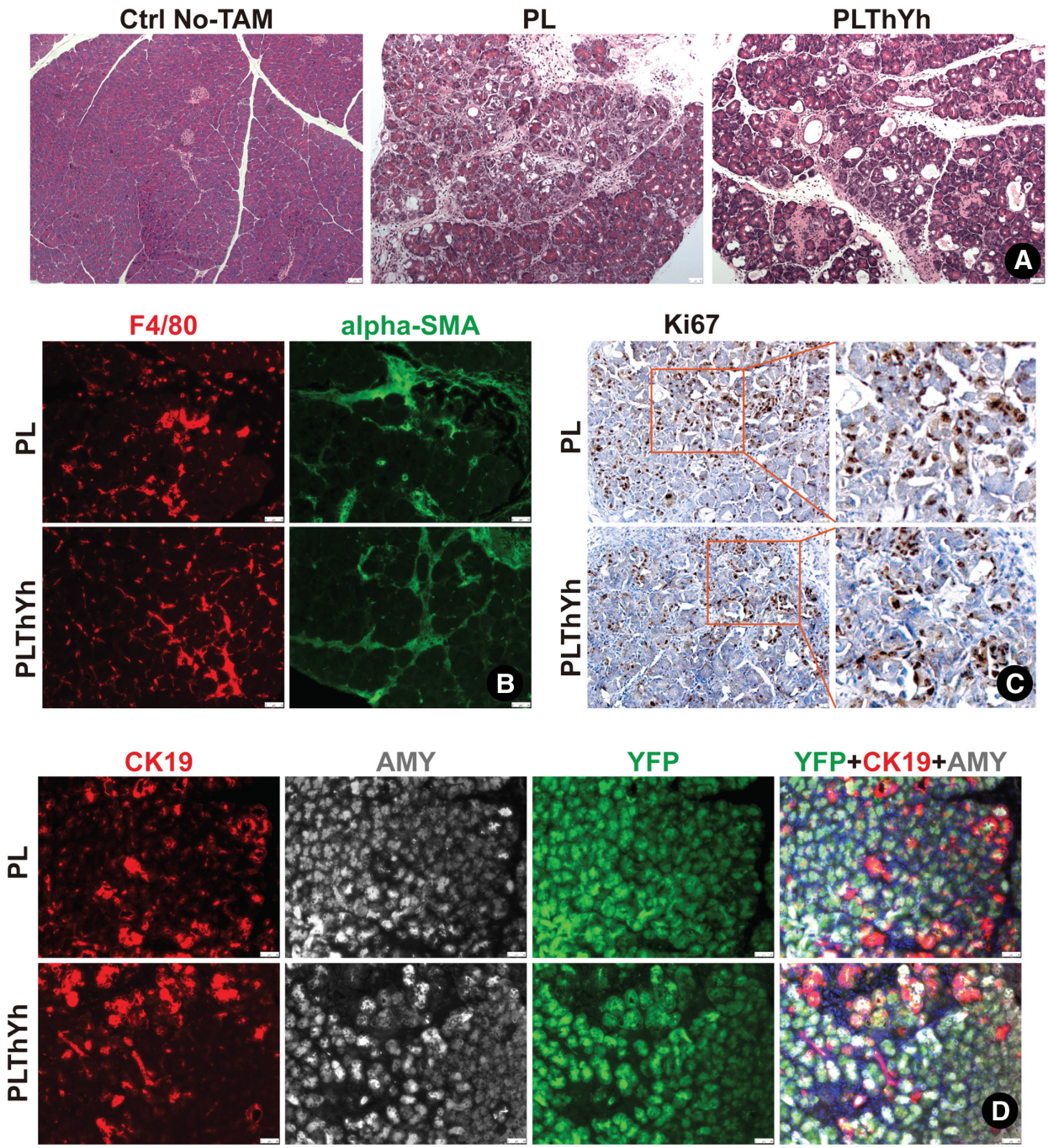

Figure 2. The pancreatic inflammation and damage caused by acinar-specific LATS1/2 knockout were not mitigated by the haplotype of YAP1 and TAZ. (A) The representative H&E staining images of the pancreas collected from the mice treated as indicated. (B) The representative IF images of F4/80 and α-SMA in the pancreas collected from PL and PLT^{Hert}Y^{Hert} mice 7 d after final TAM administration. (C) The representative IHC images of Ki67 in the pancreas collected from PL and PLY mice 7 d after final TAM administration. (D) The representative IF images of amylase and CK19 in the pancreas collected from PL and PLT^{Hert}Y^{Hert} mice 7 d after final TAM administration. PL mice (n = 5) and PLT^{Hert}Y^{Hert} mice (n = 7). CK19 = cytokeratin 19, H&E = hematoxylin and eosin, IF = immunofluorescence, IHC = Immunohistochemistry, LATS1/2 = large tumor suppressor 1/2, PL = Ptf1a^{CRE-ER} Lats1$^{fl/fl}$ Lats2$^{fl/fl}$ Rosa26$^{LSL-YFP}$ mice, PLY = Ptf1a^{CreER} Lats1$^{fl/fl}$ Lats2$^{fl/fl}$Yap1$^{fl/fl}$ Rosa26$^{LSL-YFP}$ mice, SMA = smooth muscle actin, TAM = tamoxifen.

YAP1. The knockout of YAP1 also significantly decreased macrophage infiltration and activation of fibroblasts revealed by immunofluorescent staining for F4/80 (Fig. 3C). Quantification of average positive fluorescent area of F4/80+ macrophages in PL mice (n = 3) and PLY mice (n = 3) showed a statistically significant decrease in macrophage recruitment. For α-SMA stain quantification, the average positive fluorescent area of α-SMA for PL and PLY mice also showed a statistically significant decrease in fibroblast activation (Fig. 3C). The PLY pancreas also had significantly fewer Ki67-positive cells compared to PL mice (Fig. 3D). In addition, the numbers of acinar cells undergoing ADM which were evaluated by green fluorescent protein (GFP), CK19, and amylase immunofluorescent co-staining was significantly less in PLY mice than PL mice, demonstrating reduced occurrence of ADM. Quantification of average ADM using triple-positive GFP/CK19/amylase cells showed that there were fewer ADM lesions in PLY pancreas compared with PL pancreas (Fig. 3E). We further examined the correlation of YAP1 activation and CK19 induction in acinar cells. We clearly identified sporadic GFP+ YAP1+ cells in PLY mice, consistent

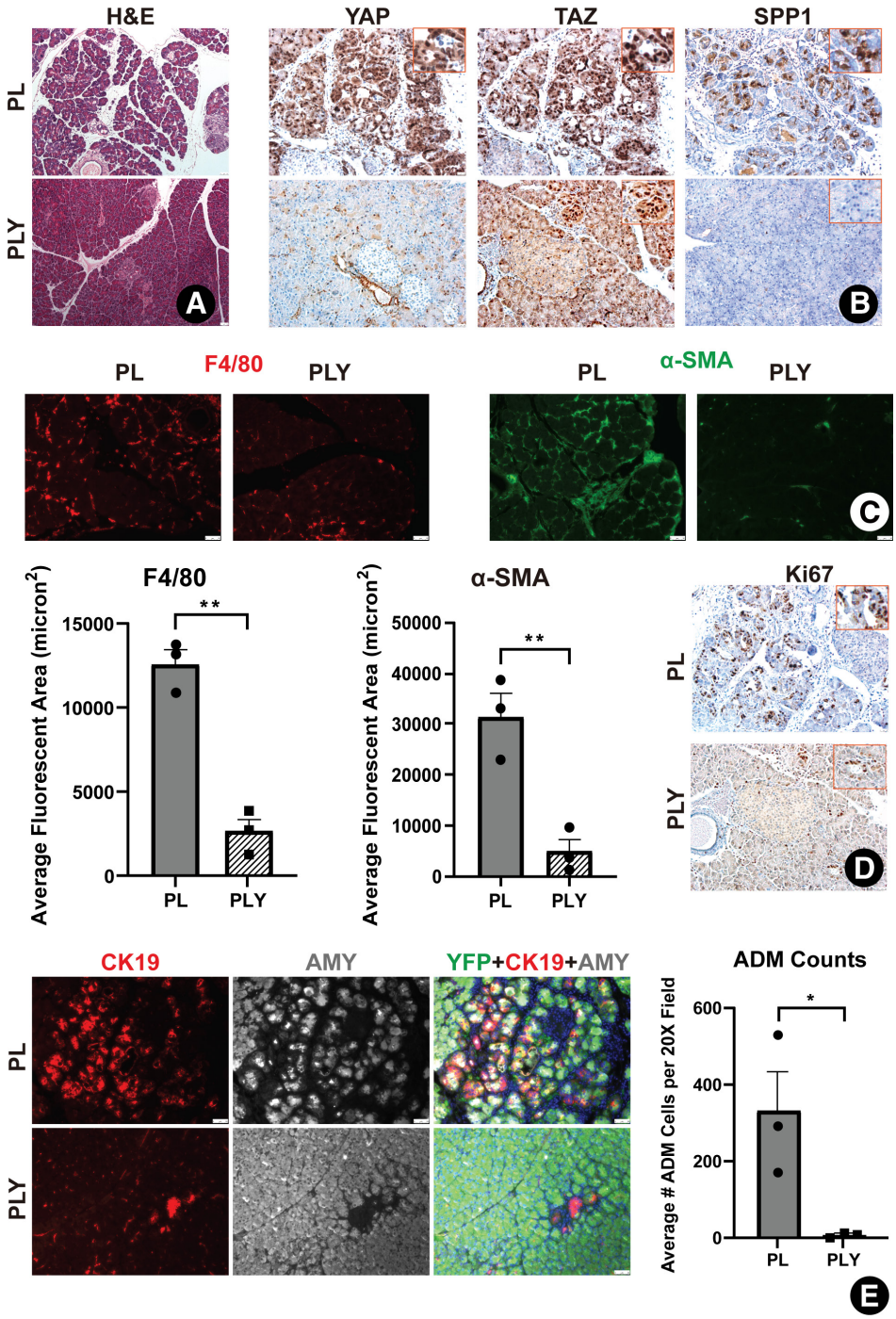

Figure 3. YAP1 is the essential mediator of the pancreatic inflammation and damages induced by LATS1/2 inactivation in acinar cells. (A) The representative H&E staining images of the pancreas collected from PL (n = 3) and PLY mice (n = 6) 7 d after final TAM administration. (B) The representative IHC images of YAP1, TAZ, and SPP1 in the pancreas collected from PL (n = 3) and PLY mice (n = 6) 7 d after final TAM administration. (C) The representative IF images of F4/80 and α-SMA in the pancreas collected from PL and PLY mice 7 d after final TAM administration. Average positive fluorescent area (in squared microns) of F4/80+ macrophage in PL mice (n = 3) was 12,624 ± 1512 while PLY mice (n = 3) was 2643 ± 1330 with *P* value = .001. The average positive fluorescent area of α-SMA for PL mice was 31,576 ± 7961 and PLY mice was 4860 ± 4315 with *P* value = .007. (D) The representative IHC images of Ki67 in the pancreas collected from PL and PLY mice 7 d after final TAM administration. (E) The representative IF images of GFP, CK19, and amylase in the pancreas collected from PL and PLY mice 7 d after final TAM administration. Quantification of average ADM numbers per 20× field using triple-positive GFP/CK19/amylase cells in PL mice was 330 ± 182.6 while PLY mice was 7 ± 6.557 with *P* value = .037. ADM = acinar to ductal metaplasia, GFP = green fluorescent protein, H&E = hematoxylin and eosin, IF = immunofluorescence, IHC = Immunohistochemistry, LATS1/2 = large tumor suppressor 1/2, PL = Ptf1a^{CRE-ER} Lats1$^{fl/fl}$ Lats2$^{fl/fl}$ Rosa26$^{LSL-YFP}$ mice, PLY = Ptf1a^{CreER} Lats1$^{fl/fl}$ Lats2$^{fl/f}$ Yap1$^{fl/fl}$ Rosa26$^{LSL-YFP}$ mice, SMA = smooth muscle actin, TAM = tamoxifen.

with the conclusion that YAP1 has not been completely ablated in all acinar cells. We did not observe any GFP+ CK19+ ADM cells without nuclear YAP1 expression, suggesting that YAP1 activation was essential for CK19 induction in acinar cells. On the other hand, we noticed that some GFP+YAP1+ cells lacked CK19 expression (Additional Fig. 2B, http://links.lww.com/JP9/A44), suggesting that additional signals might be required for YAP1 to promote CK19 expression in Lats1/2-null acinar cells. Altogether, these data suggest that YAP1 is the essential driving factor that mediates the inductive effects of acinar-specific LATS1/2 inactivation on pancreatic damage, inflammation, and ADM (Additional Fig. 3, http://links.lww.com/JP9/A45).

Homozygous TAZ knockout insignificantly reduced pancreatic inflammation and ADM induced by acinar-specific Lats1/2 deletions

Although our data demonstrated that TAZ activation in acinar cells was insufficient to cause pancreatic inflammation and damage induced by acinar-specific Lats1/2-knockout in adult mice pancreas, it remained unclear whether TAZ activation was required for these pathological alterations. To this end, we generated *Ptf1a*^{CreER}*Lats1*$^{fl/fl}$*Lats2*$^{fl/fl}$*Taz*$^{fl/fl}$*Rosa26*$^{LSL\text{-}YFP}$ (PLT) mice (Additional Fig. 1, http://links.lww.com/JP9/A43) and administered TAM as previously described to knockout LATS1/2 and TAZ. Upon histological analysis at day 6 post-TAM administration, H&E stain of PLT mice (n = 3) showed pronounced pancreatic damage and inflammation resembling PL mice (n = 3) (Fig. 4A). We evaluated the status of nuclear/cytosolic TAZ and YAP1. In the pancreas of PLT mice, nuclear YAP1 expression was seen in acinar cells, like PL mice, while TAZ expression was generally absent (Fig. 4B). In some lesions of PLT mice, nuclear TAZ expression was observed, suggesting incomplete knockouts in these cells. Nevertheless, TAZ expression was dispensable in cells within lesions (Fig. 4B). In contrast, all lesions in PLT mice clearly expressed nuclear YAP, which was consistent with nuclear YAP staining in the lesions observed in PLY mice (Fig. 3B). Additionally, IHC stains of SPP in PLT mice were closely resembled that of PL mice (Fig. 4B). Immunofluorescent stains revealed the PLT mice mimicked PL mice with increased F4/80+ macrophage infiltration and α-SMA+ fibroblast activation (Fig. 4C). The quantification of F4/80 and α-SMA stains yielded no statistically significant changes between PL and PLT mice. Similarly, the PLY pancreas also had similar numbers of Ki67-positive cells to PL mice (Fig. 4D). Next, we evaluated the occurrence of ADM by evaluating GFP, CK19, and amylase immunofluorescent co-staining as previously described. The PLT mice demonstrated similar occurrence of ADM to PL mice (Fig. 4E). Though average ADM numbers slightly decreased from PL to PLT mice, there was no statistically significant difference. We further examined the correlation of AMD with YAP1 activation. In PLT mice, nuclear YAP1 staining was present in the majority of GFP-labeled acinar cells, which was consistent with the previous IHC YAP1 stain on PLT mice (Fig. 4B). As expected, all GFP+ CK19+ ADM cells in the PLT mice expressed nuclear YAP1 (Additional Fig. 2C, http://links.lww.com/JP9/A44). Together, these data not only suggest that TAZ has a minimal effect on induction of pancreatic inflammation and is dispensable for ADM in Lats1/2-null acinar cells, but also further confirmed that YAP1 is the primary initiator and driver of these responses within the pancreas.

Pharmaceutical YAP1/TAZ-TEAD-complex inhibitor VT-104 treatment attenuates inflammation and ADM induced by acinar-specific Lats1/2 deletions

Previously, Tang et al[12] identified novel YAP/TAZ-TEAD-complex inhibitor VT-104 to be a promising and potent pharmaceutical candidate for cancer treatment due to its ability to inhibit tumor growth and proliferation of NF2-deficient mesothelioma in vitro and in xenograft in vivo models. We demonstrated the requirement of YAP1 to induce pancreatitis-like phenotypes through genetic mouse models. To further evaluate if a pharmacologic inhibition of YAP1-TEAD interaction can attenuate pancreatic inflammation and damage due to inactivation of Hippo pathway, we treated TAM-administrated PL mice with Saline (n = 3) as controls or VT-104 (n = 5) for 9 days (Fig. 5A). We used the VT-104 at the concentration of 3 mg/kg because it effectively inhibited YAP1 activation in vivo and was well-tolerated by mice without exhibiting significant side effects.[12] Expectedly, histological analysis by H&E stain revealed extensive damage to PL + saline treatment mice consistent with previous PL mice phenotypes. In contrast, the PL + VT-104 treatment mice showed significant reduction in overall pancreatic damage and inflammation (Fig. 5B). We further performed immunofluorescent stains on F4/80+ macrophage and α-SMA of activated fibroblasts, each showing significant reductions after VT-104 treatment compared to saline-treated mice, respectively. Quantification of F4/80 showed the average fluorescent area (in squared microns) for PL + saline (n = 3) was 41,338 ± 5096 while PL + VT-104 (n = 5) was 8206 ± 3601 with a *P* value of <.0001. Quantification of α-SMA showed the average fluorescent area for PL + saline was 65,252 ± 10,555 while PL + VT-104 was 20,030 ± 10,923 with a *P* value = 0.001 (Fig. 5B). We then analyzed ADM numbers using the same parameters previously described by immunofluorescent co-stains where PL + VT-104 treatment mice demonstrated significant reduction in ADM (Fig. 5C). Quantification of ADM numbers for PL + saline mice were 543.3 ± 81.45 while PL + VT-104 mice were 135.2 ± 85.27 with a *P* value = 0.001 (Fig. 5C). Altogether, these data demonstrate the robust efficacy of pharmaceutically targeted YAP/TAZ-TEAD-complex inhibition in resolving severe pancreatitis phenotypes induced by genomic-level Hippo-pathway inactivation.

Discussion

We previously reported that loss of Lats1&2 in mouse adult acinar cells led to inflammation in pancreas which can be rescued by further deletion of YAP1 and TAZ.[10] YAP1 and TAZ were originally considered as the redundant downstream mediators of Hippo pathway,[16] but subsequent studies have challenged this notion.[17] The whole-body knockout of YAP1 in mice resulted in embryonic lethal,[18] whereas the knockout of TAZ was not lethal during development, although it did lead to abnormality in certain tissues.[19] These observations underscore the importance of assessing the individual functions of YAP1 and TAZ in context-dependent manner. Here we showed that deletion of YAP1 but not TAZ can rescue the fibroinflammation caused by loss of Lats1/2. These observations demonstrated that YAP1 activation is necessary and sufficient in facilitating the changes induced by the deletions of LATS1/2 in adult pancreatic acinar cells. In addition, our data also exclude the possibility that the TAZ activation in LATS1/2-deficient acinar cells is suppressed by YAP1 knockout, suggesting that TAZ activation was neither required nor sufficient to mediate the changes induced by LATS1/2 deletions in adult pancreatic acinar cells.

The distinct consequences of YAP1 and TAZ activation reflect their differential transcriptional activities in adult pancreatic acinar cells. It is important to note that both YAP1 and TAZ need to interact with other factors to initiate transcription, as they do not bind DNA directly. The TEADS are the most well-known DNA-binding transcriptional factors (TF) that interact with YAP1 and TAZ.[6,7] However, YAP1 and TAZ may use other DNA-binding TFs to regulate gene expression.[20] While it is possible that YAP1 has TEAD-independent targets that may contribute to the induction of fibroinflammation, the earlier studies showed CTGF, a well-known TEAD-dependent target of YAP1 and TAZ, was partially responsible for it.[10,11] Consistent with this view, treatment with VT-104, a new compound which can block the interaction between TEADs and YAP1, largely rescue the pancreatic damages in mice with acinar-specific deletions of LATS1/2.These findings highlight the therapeutic potential of VT-104 for the treatment of pancreatitis. The exact mechanism why TAZ expression in acinar cells did not induce inflammatory response needs to be further investigated. In addition to binding with TEADs, YAP1 and TAZ also interact with other proteins through WW domain which recognizes PPxY motif.[21] Interestingly, YAP1 has 2 WW domains while TAZ harbors only 1 WW domain, implying that YAP1 and TAZ might differentially interact with co-factors in particular contexts.[20] It has been reported that YAP1 and TAZ are activated by phosphorylated- and dephosphorylated-parafibromin, respectively, leading to the mutually exclusive YAP or TAZ activation in mouse fibroblasts.[22] Parafibromin is a component of RNA polymerase II–associated factor 1 complex which interacts with YAP in stressed mouse pancreatic acinar

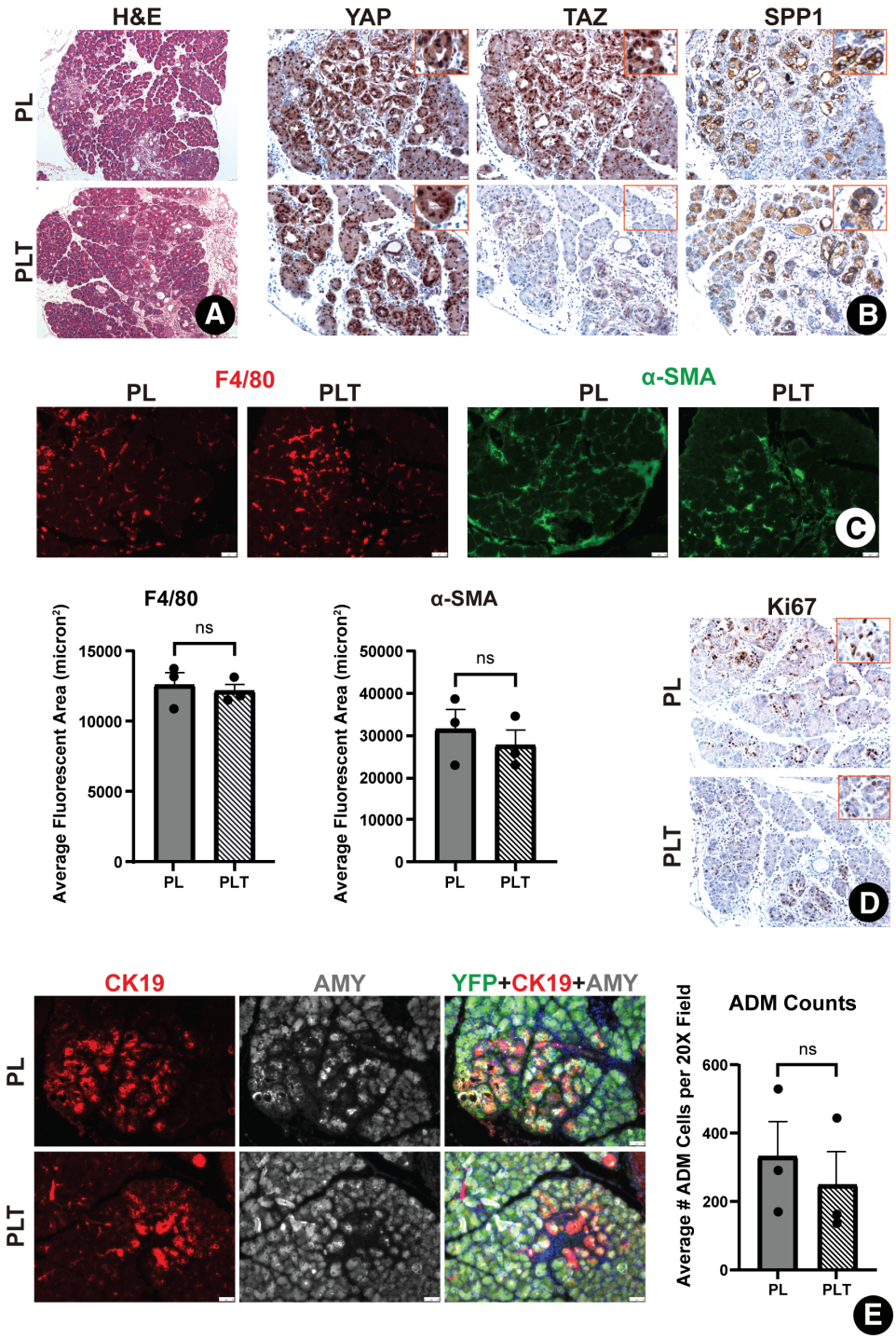

Figure 4. TAZ is dispensable for the induction of pancreatic inflammation and damages in mice with LATS1/2 deficiency in acinar cells. (A) The representative H&E staining images of the pancreas collected from PL and PLT mice 7 d after final TAM administration. (B) The representative IHC images of YAP1, TAZ, and SPP1 in the pancreas collected from PL and PLT mice 7 d after final TAM administration. (C) The representative IF images of F4/80 and α-SMA in the pancreas collected from PL and PLT mice 7 d after final TAM administration. (D) The representative IHC images of Ki67 in the pancreas collected from PL and PLT mice 7 d after final TAM administration. (E) The representative IF images of GFP, CK19, and amylase in the pancreas collected from PL and PLT mice 7 d after final TAM administration. PL mice (n = 3) and PLT mice (n = 3). CK19 = cytokeratin 19, GFP = green fluorescent protein, H&E = hematoxylin and eosin, IF = immunofluorescence, IHC = Immunohistochemistry, LATS1/2 = large tumor suppressor 1/2, PL = Ptf1a^{CRE-ER} Lats1$^{fl/fl}$ Lats2$^{fl/fl}$ Rosa26$^{LSL-YFP}$ mice, PLY = Ptf1a^{CreER} Lats1$^{fl/fl}$ Lats2$^{fl/fl}$Yap1$^{fl/fl}$ Rosa26$^{LSL-YFP}$ mice, SMA = smooth muscle actin, TAM = tamoxifen.

cells.[23] Thus, it would be interesting to investigate whether parafibromin phosphorylation status dictates the selective YAP1 activation in acinar cells.

The observation that heterozygous YAP1 knockout had minimal effects to lessen the inflammation caused by LATS1/2 deficiencies, suggesting that the acinar cells are highly sensitive to YAP1 activation, which should be tightly controlled in physiological conditions. Indeed, in the absence of stresses, no detectable pancreatic abnormalities were observed at either 1 week or 4 months after YAP1 and TAZ knockout in pancreatic acinar cells. On the other hand, aberrant YAP1 activation in acinar-derived cells has been observed under various disease scenarios including pancreatitis and pancreatic cancer.[14,15,24] Therefore, it is crucial to delve deeper into the roles of YAP1

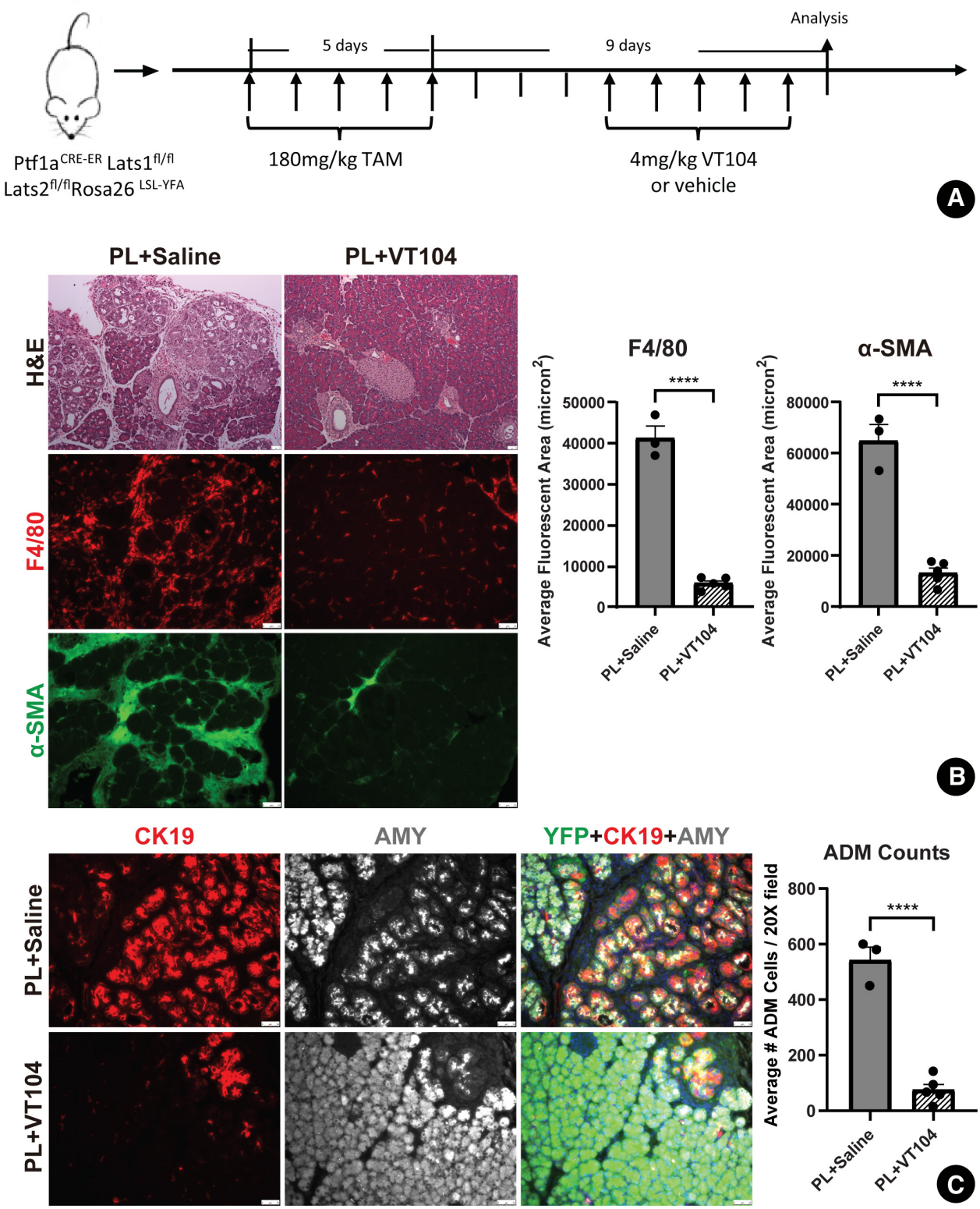

Figure 5. Yap1/Taz pharmaceutic inhibitor VT-104 ameliorate pancreatic damages induced by Lats1/2 ablation. (A) The schema of VT-104 treatment procedure. (B) The representative H&E staining images of the pancreas collected from saline-treated and VT-104-treated mice 7 d after final TAM administration. (C) The representative IF images of F4/80 and α-SMA in the pancreas collected from saline-treated and VT-104-treated mice 7 d after final TAM administration. (D) The representative IF images of GFP, CK19, and amylase in the pancreas collected from saline-treated and VT-104-treated mice 7 d after final TAM administration. Saline-treated mice (n = 3) and V-T104-treated mice (n = 5). CK19 = cytokeratin 19, GFP = green fluorescent protein, H&E = hematoxylin and eosin, IF = immunofluorescence, SMA = smooth muscle actin, TAM = tamoxifen.

activation and investigate how it is exploited to facilitate disease progression. The roles of YAP1 in driving ADM remain controversial. One previous study suggested that YAP1 activation is sufficient to induce ADM.[14] This conclusion, however, relied partially on observations from in vitro culture models. In our in vivo genetic models, we observed that some acinar cells with nuclear YAP1 did not express CK19, suggesting additional factors are also required to induce typical ADM. However, the

observation that all acinar-derived CK19-positive cells displayed nuclear localization of YAP1 emphasized the important contributions of YAP1 activation to ADM phenotypes. Interestingly, previous studies have reported that in the pancreatic cancer model, oncogenic KRAS perpetuated the acute injury–induced ADM in YAP1-dependent manner.[25,26] In conjunction with the observation that oncogenic KRAS can stabilize YAP1 activation at post-translation level,[25] these data suggested that YAP1 activation played the key roles in stabilizing the duct-like phenotypes in ADM lesions.

In summary, the strengths of our present study lie in the development of multiple genetic models to systemically evaluate the roles of Yap1 and Taz in driving the pancreatic pathological changes resulting from the disruption of the Hippo pathway within pancreatic acinar cells. Additionally, we explored the potential of mitigating these alterations through pharmaceutical inhibition of the transcriptional activity of Yap1/Taz. Therefore, aside from clarifying the distinct roles of Yap1 and Taz in acinar cells and shedding light on understanding the roles of Yap1 in ADM development, a crucial alternation in pancreatic disease progression, our research also lays the groundwork for the rationale for pharmaceutically targeting Yap1 as a promising strategy to treat pancreatic diseases. We also noticed the limitations of the current research. First, although we demonstrated that YAP1 and TAZ are not required to maintain pancreas homeostasis under physiological conditions, it is unclear whether their transient activation contributes to tissue regeneration upon acute pancreatic injuries. This information should be important to determine the appropriate timing of YAP1/TAZ inhibition for pancreatitis treatment. Second, the mechanisms differentially regulating the transcriptional activities of YAP1 and TAZ in pancreatic acinar cells remain unclear. Third, the current study examined the pharmaceutical potential of VT-104 in PL mice. This genetic model may not recapitulate all features of CP. Therefore, further studies are required to evaluate the effectiveness of VT-104, either independently or in combination with other agents, in experimental CP models.

Acknowledgments

None.

Author contributions

Conceptualization: PW, JL. Data curation: KL, JJD, YX. Formal analysis: KL, JL FES, YX. Funding acquisition: PW, JL. Methodology: KL, JL FES, YX. Project administration: PW, JL. Supervision: PW, JL. Writing – original draft: KL, PW, JL. Writing – review & editing: PW, JL, YX.

Financial support

PW is a CPRIT scholar. This work is supported by the Cancer Prevention and Research Institute of Texas (PW, no. R1219), NIDDK (PW, no. R01DK110361), and DOD (JL, no. E01 W81XWH211007). The funders had no role in study design, data collection and analysis, decision to publish, or preparation of the manuscript.

Conflicts of interest

The authors declare no conflicts of interest.

Ethics approval

All animal study protocols were approved by the University of Texas Health San Antonio Animal Care and Use Committee (Approval number: IACUC-20200099AR, and approval date: 02/24/2021).

References

[1] Lee PJ, Papachristou GI. New insights into acute pancreatitis. Nat Rev Gastroenterol Hepatol. 2019;16:479–496.
[2] Sankaran SJ, Xiao AY, Wu LM, et al. Frequency of progression from acute to chronic pancreatitis and risk factors: a meta-analysis. Gastroenterology. 2015;149:1490–1500.e1.
[3] Ali UA, Issa Y, Hagenaars JC, et al. Risk of recurrent pancreatitis and progression to chronic pancreatitis after a first episode of acute pancreatitis. Clin Gastroenterol Hepatol. 2016;14:738–746.
[4] Afghani E, Pandol SJ, Shimosegawa T, et al. Acute pancreatitis—progress and challenges: a report on an international symposium. Pancreas. 2015;44:1195–1210.
[5] Meng Z, Moroishi T, Guan K-L. Mechanisms of Hippo pathway regulation. Genes Dev. 2016;30:1–17.
[6] Plouffe SW, Meng Z, Lin KC, et al. Characterization of Hippo pathway components by gene inactivation. Mol Cell. 2016;64:993–1008.
[7] Cunningham R, Hansen CG. The Hippo pathway in cancer: YAP/TAZ and TEAD as therapeutic targets in cancer. Clin Sci (Lond). 2022;136:197–222.
[8] Ma S, Meng Z, Chen R, et al. The Hippo pathway: biology and pathophysiology. Annu Rev Biochem. 2019;88:577–604.
[9] Wang S, Zhou L, Ling L, et al. The crosstalk between Hippo-YAP pathway and innate immunity. Front Immunol. 2020;11:323.
[10] Liu J, Gao M, Nipper M, et al. Activation of the intrinsic fibroinflammatory program in adult pancreatic acinar cells triggered by Hippo signaling disruption. PLoS Biol. 2019;17:9.
[11] Tamura T, Kodama T, Sato K, et al. Dysregulation of PI3K and Hippo signaling pathways synergistically induces chronic pancreatitis via CTGF upregulation. J Clin Invest. 2021;131:e143414.
[12] Tang TT, Konradi AW, Feng Y, et al. Small molecule inhibitors of TEAD auto-palmitoylation selectively inhibit proliferation and tumor growth of NF2-deficient mesothelioma. Mol Cancer Ther. 2021;20:986–998.
[13] George NM, Day CE, Boerner BP, et al. Hippo signaling regulates pancreas development through inactivation of Yap. Mol Cell Biol. 2019;32:5116–5128.
[14] Gruber R, Panayiotou R, Nye E, et al. YAP1 and TAZ control pancreatic cancer initiation in mice by direct up-regulation of JAK-STAT3 signaling. Gastroenterology. 2016;151:526–539.
[15] Kapoor A, Yao W, Ying H, et al. Yap1 activation enables bypass of oncogenic Kras addiction in pancreatic cancer. Cell. 2014;158:185–197.
[16] Plouffe SW, Lin KC, Moore JL, et al. The Hippo pathway effector proteins YAP and TAZ have both distinct and overlapping functions in the cell. J Biol Chem. 2018;293:11230–11240.
[17] Luo J, Li P. Context-dependent transcriptional regulations of YAP/TAZ in stem cell and differentiation. Stem Cell Res Ther. 2022;13:10.
[18] Morin-Kensicki EM, Boone BN, Howell M, et al. Defects in yolk sac vasculogenesis, chorioallantoic fusion, and embryonic axis elongation in mice with targeted disruption of Yap65. Mol Cell Biol. 2006;26:77–87.
[19] Makita R, Uchijima Y, Nishiyama K, et al. Multiple renal cysts, urinary concentration defects, and pulmonary emphysematous changes in mice lacking TAZ. Am J Physiol Renal Physiol. 2008;294:F542–F553.
[20] Reggiani F, Gobbi G, Ciarrocchi A, et al. YAP and TAZ are not identical twins. Trends Biochem Sci. 2021;46:154–168.
[21] Chen Y-A, Lu C-Y, Cheng T-Y, et al. WW domain-containing proteins YAP and TAZ in the Hippo pathway as key regulators in stemness maintenance, tissue homeostasis, and tumorigenesis. Front Oncol. 2019;9:60.
[22] Tang C, Takahashi-Kanemitsu A, Kikuchi I, et al. Transcriptional coactivator functions of YAP and TAZ are inversely regulated by tyrosine phosphorylation status of parafibromin. iScience. 2018;1:1–15.
[23] Nimmakayala RK, Ogunleye AO, Parte S, et al. PAF1 cooperates with YAP1 in metaplastic ducts to promote pancreatic cancer. Cell Death Dis. 2020;13:839.
[24] Kapoor A, Yao W, Ying H, et al. Yap1 activation enables bypass of oncogenic Kras addiction in pancreatic cancer. Cell. 2019;179:1239–1197.
[25] Zhang W, Nandakumar N, Shi Y, et al. Downstream of mutant KRAS, the transcription regulator YAP is essential for neoplastic progression to pancreatic ductal adenocarcinoma. Sci Signaling. 2014;7:ra42.
[26] Tu B, Yao J, Ferri-Borgogno S, et al. YAP1 oncogene is a context-specific driver for pancreatic ductal adenocarcinoma. JCI Insight. 2019;4:e130811.

How to cite this article: Lopez K, Deng JJ, Xu Y, Sharkey FE, Wang P, Liu J. Exploring the role of YAP1 and TAZ in pancreatic acinar cells and the therapeutic potential of VT-104 in pancreatic inflammation. J Pancreatol 2025;8:32–40. doi: 10.1097/JP9.0000000000000170